

## RobotSLAM: A Lightweight Low-cost 3D LiDAR SLAM Handheld Device

Huimin Gao<sup>1</sup>, Gefei Kong<sup>2</sup>, Xiaochuan Huang<sup>3</sup>, Hongchao Fan<sup>4</sup>, Ruofei Zhong<sup>5</sup>

<sup>1</sup> College of Resources, Environment and Tourism, Capital Normal University, Beijing, P.R. China – 543177458@qq.com

<sup>2</sup> Department of Civil and Environmental Engineering, Norwegian University of Science and Technology, Trondheim, Norway – gefei.kong@ntnu.no

<sup>3</sup> Zhengtu 3D (Beijing) Laser Technology Co., Ltd., Beijing, P.R. China – peterdachuan@126.com

<sup>4</sup> Department of Civil and Environmental Engineering, Norwegian University of Science and Technology, Trondheim, Norway – hongchao.fan@ntnu.no

<sup>5</sup> College of Resources, Environment and Tourism, Capital Normal University, Beijing, P.R. China – zrfss@163.com

**Keywords:** Mobile Laser Scanning (MLS), Handheld Device, Simultaneous Localization and Mapping (SLAM), Multi-sensor Fusion, Point Cloud Accuracy Verification.

### Abstract

As the importance of Mobile Laser Scanning (MLS) technology in 3D mapping continues to grow, the development of low-cost, portable devices to address the complex mapping needs of various environments has become a key area of research in the industry. Currently, handheld MLS devices are increasingly being applied in a wide range of surveying tasks, especially in small outdoor spaces, indoor environments, and narrow areas with limited accessibility. This study proposes the development of a novel handheld mobile laser scanning system, *RobotSLAM Lite*. The system integrates a LiDAR sensor and a fisheye camera through a multi-sensor fusion approach to enable Simultaneous Localization and Mapping (SLAM). A dedicated data processing platform, *RobotSLAM Engine*, has also been developed to generate and optimize point cloud maps with true-color information. To evaluate the system's performance, the study was conducted at the Norwegian University of Science and Technology, utilizing an experimental building and nearby roads as test sites. High-precision point cloud data obtained from a terrestrial laser scanner (Leica ScanStation P30 TLS) and RTK measurement Ground Control Points (GCPs) were used as reference benchmarks. A four-metric evaluation framework, comprising absolute coordinate deviation, point cloud density distribution, surface roughness, and cloud-to-cloud distance (C2C), was established to quantitatively analyze the mapping accuracy of the device in indoor and outdoor scenarios at various scales. Experimental results indicate that *RobotSLAM Lite* provides centimeter-level accuracy while significantly reducing both equipment cost and operational complexity, offering a new technological solution for 3D mapping in both large and small spaces.

### 1. Introduction

In traditional laser surveying, terrestrial laser scanners (TLS) have long served as the core method for high-precision 3D spatial data acquisition. However, these technologies exhibit significant operational limitations: firstly, TLS requires line-of-sight conditions to establish control networks, resulting in restricted coverage per station; additionally, the equipment necessitates collaborative operation by specialized personnel, leading to increased labor intensity for field staff.

To overcome these technical bottlenecks, Mobile Laser Scanning (MLS) devices have emerged. Mobile surveying solutions, by ensuring point cloud accuracy and data integrity, substantially enhance field data collection efficiency. This leap in efficiency is attributed to their unique dynamic scanning mechanism—eliminating the time-consuming relocation between fixed stations, thereby enabling continuous 3D data acquisition.

Laser scanning technology is increasingly evolving towards dynamic and large-scale applications, which is a great transformation driven by the development of MLS, Airborne Laser Scanning (ALS) and Simultaneous Localization and Mapping (SLAM). These technologies are widely applied in various disciplines, including autonomous driving, forestry investigation, and urban 3D modeling (Cadena, C. et al, 2016). To facilitate broader adoption in these areas, recent advancements in LiDAR technology have focused on reducing device costs while enhancing its reliability and flexibility (Lin,

J. and Zhang, F. 2020). Unlike traditional MLS that typically rely on large platforms such as vehicles or aircraft, Personal/Portable Laser Scanner (PLS) (Di Stefano, F. et al., 2021), such as handheld PLS, place the consumer-grade laser scanners on portable equipment. These devices are suitable for more flexible 3D data collection in small-scale scenes, particularly in complex terrains and narrow spaces, and indoor scenes.

This study develops *RobotSLAM Lite*, a lightweight, low-cost 3D LiDAR handheld device. While ensuring affordability and portability, the device achieves high accuracy and vivid color mapping across both small- and large-scale environments, including indoor and outdoor settings. Additionally, an accompanying software platform, *RobotSLAM Engine*, has been developed for this device, which supports efficient computation, visualization, and processing of point cloud data with advanced functionalities.

To comprehensively validate the performance of this device, this study selected two scenes for case studies: (1) the main roads around Norwegian University of Science and Technology (NTNU) as a large-scale outdoor scene, and (2) the corridors of a building at NTNU as a small indoor scene. High-precision point clouds obtained from the Leica ScanStation P30 terrestrial laser scanner (TLS) and control points collected with Leica Real-time Kinematic (RTK) were used as reference data. The evaluation metrics—absolute coordinates, point cloud density, surface roughness, and cloud-to-cloud distance (C2C)—will be used to verify the point cloud quality collected by *RobotSLAM*.

## 2. Product Design and Innovation

### 2.1 Hardware (*RobotSLAM Lite*)

*RobotSLAM Lite* handheld mobile scanning system developed in this study employs a multi-source heterogeneous sensor fusion architecture to achieve a synergistic optimization of lightweight design and high-precision 3D data acquisition. As shown in Figure 1, the system hardware configurations are as follows:

**2.1.1 Sensor Unit:** The Laser Scanning Module is equipped with the DJI Livox Mid-360 hybrid-solid LiDAR sensor, built in an Inertial Measurement Unit (IMU), which utilizes non-repetitive scanning technology to achieve a composite field of view (FoV) of  $360^\circ$  (horizontal)  $\times$   $59^\circ$  (vertical). At a reference distance of 10 meters, the ranging accuracy reaches 2 cm ( $1\sigma$  confidence interval), with angular accuracy better than  $0.15^\circ$  (RMS), and an effective detection range spanning 0.1 to 70 meters, meeting the surveying requirements in most scenarios. The Panoramic Imaging Module integrates a dual-fisheye lens panoramic camera system, with a total weight of 135 grams. The front and rear lens groups are arranged back-to-back to achieve  $360^\circ$  omnidirectional coverage. Each lens supports image capture at a resolution of  $6080 \times 3040$  pixels. An integrated six-axis MEMS gyroscope ensures temporal and spatial synchronization between images and point clouds.

**2.1.2 Optimized Structural Design:** The device body features a topologically optimized magnesium-aluminum alloy frame, balancing structural rigidity and lightweight design (total weight of 1.32 kg). The bottom is equipped with an arrow-shaped stabilizing base, with the tip featuring a hollow target marker (aperture of  $3 \text{ mm} \pm 0.1 \text{ mm}$ , positioning accuracy of  $\pm 0.5 \text{ mm}$ ), supporting rapid total station co-location. The handle's contact surface is ergonomically designed and made of high-friction silicone material to ensure device stability during operation, making it comfortable to use for long time data collection sessions (over 20 minutes).

**2.1.3 Intelligent Operation System:** The system is equipped with an embedded interactive control unit, enabling full-process automation:

**One-Button Acquisition:** A single press triggers simultaneous start and stop of multiple sensors. The SLAM algorithm, based on LiDAR-inertial initialization strategy, achieves convergence in less than 15 seconds.

**Status Visualization:** The display screen provides real-time status updates, including initialization, data acquisition, data saving, and sleep mode (low-power mode).

**2.1.4 High-Reliability Storage and Endurance:** Under typical power consumption (LiDAR + IMU + panoramic camera operating continuously), the system supports  $\geq 2.5$  hours of continuous scanning. The data storage unit is equipped with a 1 TB solid-state drive (sustained write speed  $\geq 500 \text{ MB/s}$ ), accommodating the maximum data volume per task (point cloud + images  $\leq 800 \text{ GB}$ ).

These configurations ensure that *RobotSLAM Lite* delivers high-precision, efficient, and user-friendly performance for 3D data acquisition in various environments.

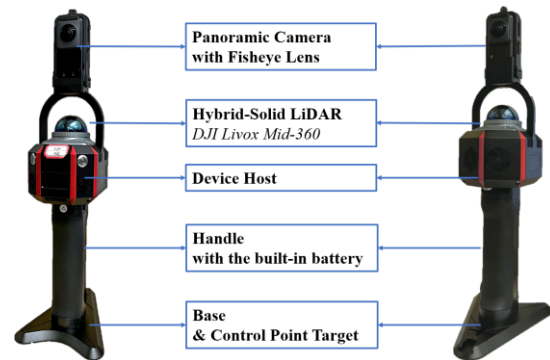


Figure 1. The Structure of *RobotSLAM Lite* (Front and Back).

### 2.2 Software (*RobotSLAM Engine*)

*RobotSLAM Engine* is based on SLAM algorithm and multi-sensor fusion, providing state estimation and obtaining real-color 3D point cloud map. Figure 2. illustrates the core software functionality distribution of *RobotSLAM Engine*, which is divided into three main modules: Point Cloud Processing, Image Processing, and SLAM Processing. The functions within each module are as follows:

**2.2.1 Point Cloud Processing:** This module includes conventional functions, coord transformation, filter, and classification for point clouds. Conventional Functions includes standard point cloud processing tools such as 3D measurements, point cloud slicing, file format conversion, point cloud rendering, resampling, and more. Coord Transformation provides 4-parameter and 7-parameter transformations to convert the point cloud data from the local coordinate system to global geographical coordinate system, ensures that the data can provide reliable and useful geographical reference information. As for Filter, the Progressive Morphological Filter (PMF) and Statistical Outlier Removal Filter (SORF) help remove noise from the point cloud, while the Cloth Simulation Filter (CSF) separates ground and non-ground point cloud data. Classifier has built-in basic point cloud categories and also supports adding categories, which requires manual operation.

**2.2.2 Image Processing:** This module calculates the pose information of the camera capturing the images, allowing point clouds to be projected onto the images and providing RGB information for coloring the point clouds.

**2.2.3 SLAM Processing:** In this module, the FAST-LIO2 (Xu, W., et al, 2022) algorithm is employed as the SLAM front-end framework. FAST-LIO2 is a fast, robust, and versatile LiDAR-inertial odometry framework that directly registers raw points to the map without feature extraction, enabling the exploitation of environmental features to enhance accuracy. Afterward, Trajectory Adjustment optimizes the device's movement trajectory to improve localization accuracy. Loop Closure feature corrects position drift by detecting overlapping regions in the point cloud data, enabling accurate map reconstruction, while GNSS coordinates can also be used outdoors to adjust the trajectory. Manual Matching allows for manual frame-to-frame matching, where the software automatically computes poses for trajectory optimization. After multiple or repeated scans, project merging can be performed, followed by global point cloud optimization. This solves issues of inconsistent data accuracy across multiple scans and enables manual alignment and registration of different datasets for accurate point cloud stitching.

These integrated functional modules enable efficient point cloud processing, precise pose estimation, and effective SLAM algorithm application, resulting in high-quality MLS and data collection.

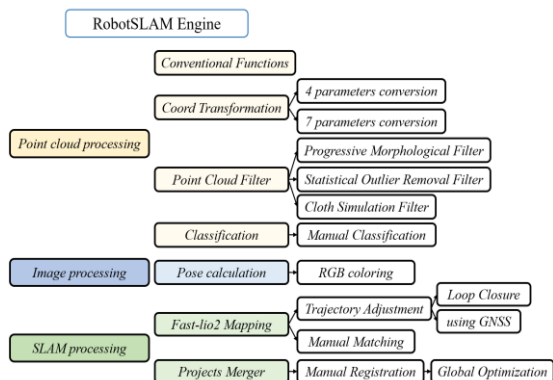


Figure 2. Modules and Functions of *RobotSLAM Engine*.

### 3. Point Cloud Data Acquisition

#### 3.1 Data Acquisition

In order to comprehensively evaluate the accuracy of the device, this study has designed the data acquisition and accuracy verification methods for both large-scale outdoor road and small-scale indoor scenarios. These environments include both typical and challenging, hard-to-handle features.

**3.1.1 Outdoor Data Acquisition:** Main roads in NTNU and surrounding area were selected for the outdoor large-scale survey, covering nearly 7000 m, with a total area of nearly 81,000 m<sup>2</sup>, as shown in Figure 3, the red lines. The road terrain in this area is relatively complicated, with significant changes in slope. Therefore, we divided the road into multiple closed loops during point cloud data acquisition, ensuring consistency between the start and end points of each loop. Each individual trajectory underwent loop closure optimization. Adjacent loops overlapped to ensure accurate stitching of the multiple routes.

**3.1.2 Indoor Data Acquisition:** The indoor data was collected in an experimental building at NTNU. The building has two floors and features numerous long corridors, with the longest measuring 69.24 m. The similar structures included in this test area makes SLAM computations highly prone to degradation and distortion. The total length of the corridors we collected is approximately 395.21 m, with 130.11 m on the first floor and 265.10 m on the second floor. In the indoor data acquisition strategy, four distinct routes were established: Firstly, data collection along the circular corridor on the first floor; next, the staircase connecting different floors, and finally, the two circular corridors on the second floor. Each route was designed to ensure approximately 30% overlap with adjacent routes, facilitating accurate alignment and integration of the point cloud data.

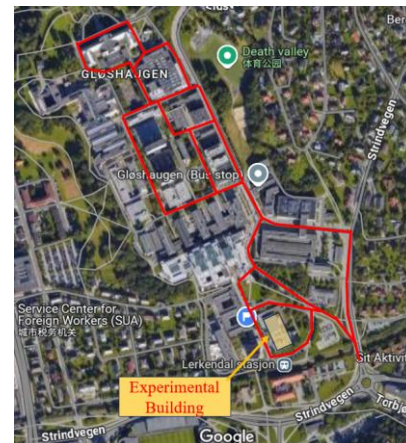


Figure 3. Experimental Area and Data Collection Routes. Statement: Screenshot from Google Maps, Time: 2025-2-10. The citation of Google Maps (<https://www.google.com/maps/>) in this study is in accordance with its terms of use and is for academic research purposes only.

#### 3.2 Data Processing

**3.2.1 Point Cloud Registration:** During the data acquisition process, nine trajectory routes and corresponding point cloud datasets were generated for the outdoor environment, while four trajectory routes and point cloud datasets were obtained for the indoor environment. In the *RobotSLAM Engine* software, each individual trajectory underwent optimization using the loop closure detection feature. Subsequently, the multi-project trajectory stitching function was employed to manually register all outdoor trajectories and all indoor trajectories, followed by global adjustment.

**3.2.2 Point Cloud Data Optimization:** After completing the global point cloud stitching, optimization procedures were applied to enhance the data quality. Initially, RGB coloring was applied to the global point cloud. Subsequently, the Statistical Outlier Removal Filter (SORF) was utilized to eliminate noise points, for the road data, primarily targeting dynamic objects such as pedestrians, vehicles, and cyclists; while for the indoor data, targeting specifically points that are reflected from glass surfaces. The parameters were set with a standard deviation multiplier ( $\alpha$ ) of 2.0 and a neighborhood size (K) of 30 for road scene and ( $\alpha$ ) of 1.5 and (K) of 20 for corridor scene.

**3.2.3 7-Parameter Transformation:** Due to the absence of RTK functionality in *RobotSLAM Lite*, it was necessary to perform a 7-parameter transformation to obtain absolute coordinates for the outdoor road point cloud. The Norwegian Public Roads Administration provided 11 high-precision Ground Control Points (GCPs) within the survey area, each with an accuracy exceeding 0.5 cm. After establishing corresponding points in the point cloud, a 7-parameter transformation was conducted, resulting in a mean error of 0.1452 m, which meets the required accuracy standards.

Totally, in the outdoor large-scale scene, we collected a total of 17.12 GB of road point cloud data, while in the indoor scene, we collected 2.22 GB of data. As shown in Figure 4 (a) and (b), the point cloud is colored by elevation, with different colors on the road surface indicating elevation changes, while Figure 4 (c) and (d) show the layout of the corridors on the first and second floors of the building, respectively.

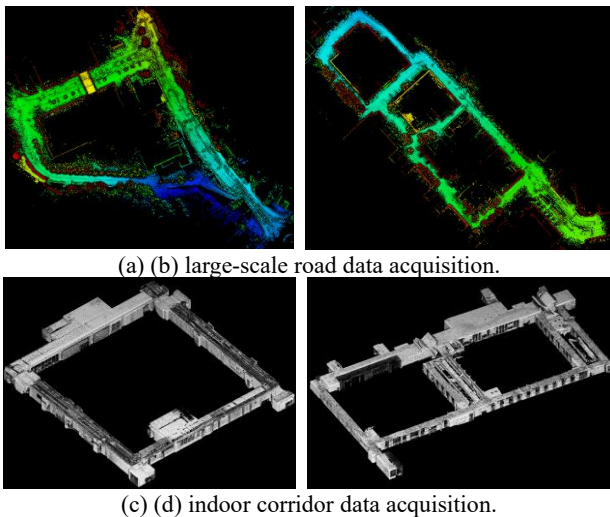


Figure 4. Display of Point Cloud Data by *RobotSLAM*.

#### 4. Data Accuracy Verification

##### 4.1 Data Accuracy Verification

The 3D TLS instruments have wide fields of view and can generate very dense and high-precision 3D point clouds, as well as they can survey roads and buildings almost non-destructively (Bi, S. et al, 2020). Therefore, in this paper, the point cloud data scanned by the Leica ScanStation P30 TLS (Leica Geosystems, Hexagon, Germany), will serve as the reference data to verify the accuracy of data scanned by *RobotSLAM*. Table 1. shows the comparison between the 2 devices. We collected data from the same road and partial data from the second floor of the

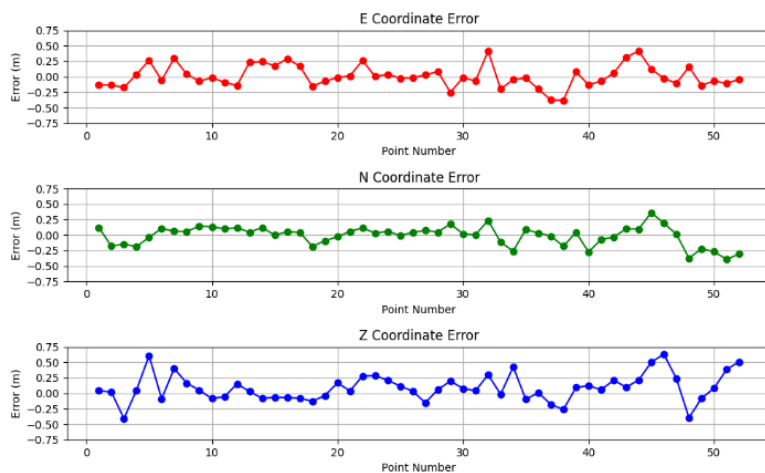
experimental building using the Leica ScanStation P30 TLS. The outdoor data from the P30 was then processed and optimized. The resulting errors are as follows: C2C Error = 0.008m; GCPs Error = 0.033m; Global Bundle Error = 0.019m.

Parameter	RobotSLAM Lite	Leica ScanStation P30
Detection Range	40m (@10% Reflectivity) 70m (@80% Reflectivity)	120m (@18% Reflectivity)
Distance Accuracy	2cm (@10m)	1.2 mm + 10 ppm
Angular Accuracy	≤ 0.15°	≤ 0.002°
Field of View	H 360°; V 59°	H 360°; V 290°
Measurement Rate	200,000 pts/s	1,000,000 pts/s

Table 1. Comparison of Device Parameters.

Here are several evaluation metrics used in this work.

**4.1.1 Absolute Coordinate Errors:** In the road scenario, 52 GCPs were selected uniformly, and their Easting (E), Northing (N), and Height (H) values were measured and recorded using a Leica GS15 GNSS Antenna Surveying RTK system. These GCPs, with the accuracy of 1-3 cm, were used to evaluate the accuracy of the absolute coordinates obtained from the handheld system. In the road point cloud with absolute coordinates, corresponding points from the GCPs are selected, and errors in the E, N, and H directions are calculated. The Mean and RMSE values are then computed. As shown in Figure 5, (a) illustrates the distribution of GCPs within the survey area, while (b) displays the error distribution in the E, N, and H directions.



(a) the distribution of GCPs; (b) the error distribution in the N, E, and H directions.

Figure 5. The Result of Absolute Coordinate Errors.

As shown in Table 2, the mean absolute error (MAE) values in the E, N, and H directions are all less than 0.2m, and the root mean square error (RMSE) values are all below 0.3m, which meets the general accuracy requirements for road surveying. As seen in Figure 5(b), the errors in the E, N, H directions are predominantly in the range of -0.25 m to 0.25 m. The errors in the horizontal (E and N) directions are smaller, while those in the H direction are more scattered. This is due to the significant elevation differences in the survey area, and the LiDAR's lower resolution and smaller field of view in the H direction compared

to the horizontal directions.

Items	E	N	H
MAE	0.136m	0.121m	0.177m
RESE	0.177m	0.256m	0.220m

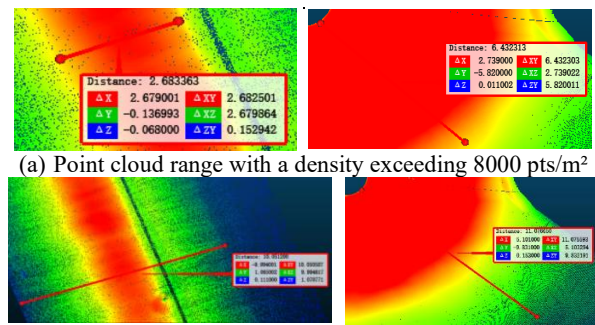
Table 2. Mean Error and RESE Values in 3 Directions.

**4.1.2 Point cloud density:** In this paper, surface density was as the point cloud density indicator, with the local neighborhood radius of 0.5642 m, to calculate the point cloud density value

within 1 m<sup>2</sup> neighborhood range. Point clouds were extracted from 15 sections of the road and building surfaces, and the surface density for each slice was calculated for analyzing their density and distribution.

As shown in Figure 6 and 7(a), (b), and (c), the point cloud data collected by *RobotSLAM Lite* exhibits a distinct variation in surface point cloud density. Specifically, the point cloud density shows consistent behavior along the direction of the scanning trajectory, while it exhibits a gradient change in the direction perpendicular to the trajectory. As the distance from the trajectory points increases, the point cloud density decreases. Within 10-meter near the trajectory routes, the point cloud density reaches 1500 pts/m<sup>2</sup>, while within 3 meters of the trajectory, the density increases significantly, exceeding 8000 pts/m<sup>2</sup>. This variation in point cloud density reflects the scanning system's capacity to capture more detailed information near the trajectory while gradually losing precision as the distance from the scanning path increases. This behavior is indicative of the

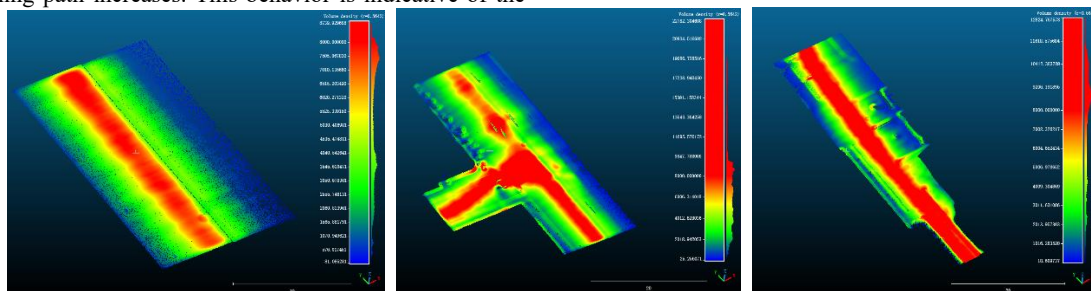
inherent properties of MLS systems.



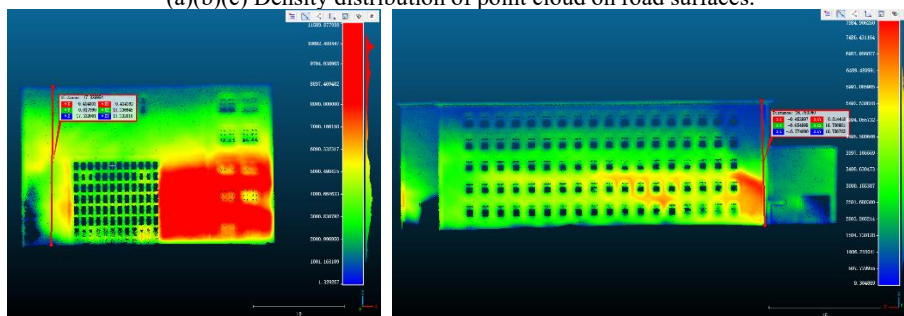
(a) Point cloud range with a density exceeding 8000 pts/m<sup>2</sup>

(b) Point cloud range with a density reaching 1500 pts/m<sup>2</sup>.

Figure 6. The Comparison of Point Cloud Density. (*RobotSLAM* on the left and Leica P30 on the right.)



(a)(b)(c) Density distribution of point cloud on road surfaces.



(d)(e) Density distribution of point cloud on building facade.

Figure 7. Some visualization results of point cloud density from *RobotSLAM*.

**4.1.3 Surface roughness:** In this paper, the definition of point cloud roughness is as follows: The point cloud roughness of point  $p$  is determined by fitting a reference plane using the points within its neighborhood. The directed distance from point  $p$  to the reference plane is considered the roughness of point  $p$  (Ma, X., et al, 2024). We have extracted point clouds from 15 sections of the road/building surfaces and 5 sections of indoor corridor scenes, including point clouds of wooden doors, white walls, and floor surfaces. For each point cloud slice, we have calculated the surface roughness and selected the same sections in the TLS point cloud for comparison.

According to Figure 8. (a)(b)(c)(d), in the indoor scene, the building corner points exhibit higher roughness, a feature observed in both devices. However, the point cloud from *RobotSLAM* exhibits significantly greater roughness (approximately 0 ~ 0.7), while the roughness of the point cloud from Leica P30 is confined to a range of 0 ~ 0.04, much smaller in comparison. In the outdoor scene (as shown in Figure 8. (e)(f)(g)(h)), the road surface captured by *RobotSLAM* exhibits good performance (roughness values approximately 0 ~ 0.05). However, in the building facade, while smooth wall surfaces yield favorable results, the roughness increases significantly at the window sills and eaves.

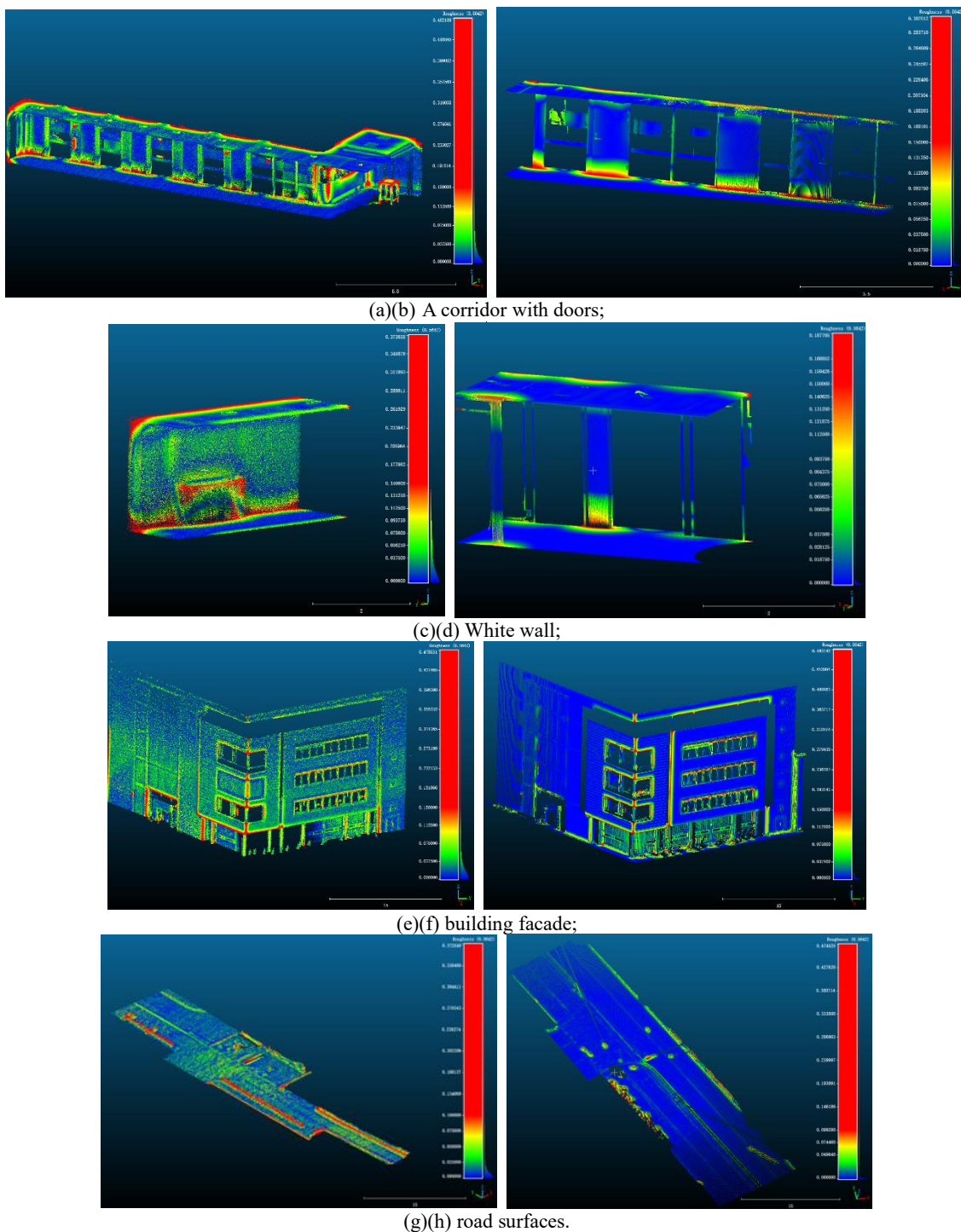
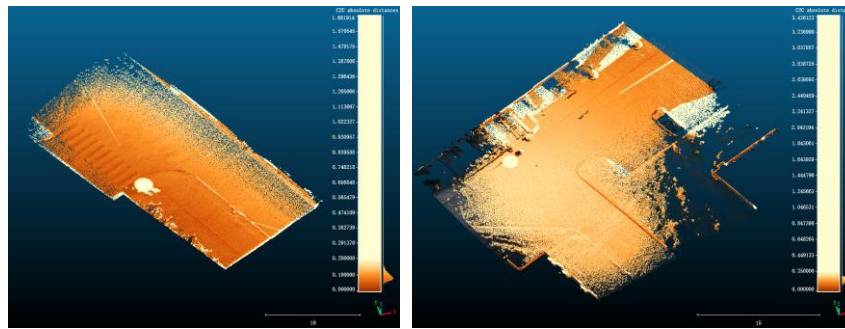


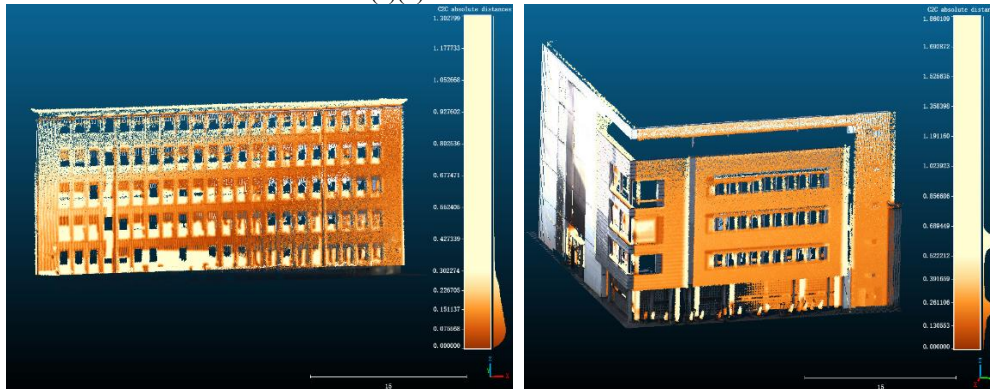
Figure 8. Some visualization results of point cloud roughness. (*RobotSLAM* left and *Leica P30* right.)

**4.1.4 Cloud-to-cloud Distance:** In outdoor scene, the cloud-to-cloud distances were calculated between the *RobotSLAM* point clouds and TLS road data. This measures the level of detail in the data construction. In the C2C calculation results for the 15 road and building surfaces, the road slices consistently yielded favorable experimental results. As shown in Figure 9. (a)(b), the amber color reflects the C2C distance values and their

distribution. The darker the color, the smaller the distance, indicating higher relative accuracy. In the road slices, the average relative distance is better than 0.2m. However, in the building facade calculations, the average relative distance is only better than 0.3m. As shown in Figure 9. (d), which represents the largest error, a distance difference of 0.5~0.7m is observed on one facade.



(a)(b) C2C in road sections.



(c)(d) C2C in building facade.

Figure 9. Some Results of C2C Distance.

## 5. Conclusion

This paper provides a detailed introduction and accuracy evaluation of the *RobotSLAM Lite*, a portable and low-cost handheld mobile laser scanning device designed and developed for surveying applications. The results indicate that, in both indoor and outdoor environments across large and small-scale scenarios, the device performs excellently in terms of point cloud coordinate accuracy and geometric precision. Based on a laser SLAM algorithm for mapping and supported by point cloud map quality optimization functions in *RobotSLAM Engine*, the *RobotSLAM Lite* performs well across several key metrics, including absolute coordinates, point cloud density, surface roughness, and cloud-to-cloud distance.

The primary advantages of the *RobotSLAM Lite* lie in its lightweight design, affordability, and ease of use, making it an attractive solution for surveying tasks in both large and small-scale environments. However, this study also highlights certain limitations of the device, such as the occurrence of significant point cloud noise in highly dynamic or cluttered environments, as well as a reduction in point cloud density. Additionally, the accuracy of point cloud coloring still requires further optimization.

Future research will focus on improving methods for dynamic object removal to ensure better point cloud quality. Currently, we are developing techniques using Gaussian splatting to enhance the fusion modelling accuracy between images and point clouds, as well as expanding its application in more complex environments.

Overall, this study underscores *RobotSLAM* as a cost-effective, multifunctional tool in modern surveying, with significant promise for widespread applications in industries such as

construction surveying, road mapping, and indoor modelling.

## Reference

- AG, L. G. 2017. Leica ScanStation P30/P40 product specifications.
- Bi, S., Chang, Y., Chang L., Jun C., Wei W., and Yueri C.. 2021. A Survey of Low-Cost 3D Laser Scanning Technology. *Applied Sciences* 11(9), 3938. [doi.org/10.3390/app11093938](https://doi.org/10.3390/app11093938).
- Cadena, C., Carlone, L., Carrillo, H., Latif, Y., Scaramuzza, D., Neira, J. 2016. Past, Present, and Future of Simultaneous Localization and Mapping: Toward the Robust-Perception Age. *IEEE Transactions on Robotics*, 32(6), 1309-1332. doi: 10.1109/TRO.2016.2624754.
- Di Stefano, F., Chiappini, S., Gorreja, A., Balestra, M., and Pierdicca, R. 2021. Mobile 3D scan LiDAR: a literature review. *Geomatics, Natural Hazards and Risk*, 12(1), 2387–2429. [doi.org/10.1080/19475705.2021.1964617](https://doi.org/10.1080/19475705.2021.1964617).
- Lin, J., and Zhang J.. Loam livox: A fast, robust, high-precision LiDAR odometry and mapping package for LiDAR of small FoV. 2020. IEEE International Conference on Robotics and Automation (ICRA), Paris, France. doi: 10.1109/ICRA40945.2020.9197440.
- Ma, X., Yue, D., Shen, Y., Liu, R., Wang, M., Yu, J., Zhang, C. 2024. Pavement Pothole Detection Method Based on Vehicle-Borne Laser Point Clouds. *Chinese Journal of Lasers*, 51(5): 0510004.
- Xu, W., Cai, W., He, D., Lin, D., and Zhang, F., 2022. FAST-LIO2: Fast Direct LiDAR-Inertial Odometry. *IEEE Transactions on Robotics*, 38(4): 2053-2073.